ACS Macro Letters

Letter

pubs.acs.org/macroletters

Polystyrene Glasses under Compression: Ductile and Brittle Responses

Jianning Liu,[†] Panpan Lin,[†] Shiwang Cheng,[‡] Weiyu Wang,[§] Jimmy W. Mays,[§] and Shi-Qing Wang*[,†]

[†]Department of Polymer Science, University of Akron, Akron, Ohio 44325, United States

[‡]Chemical Sciences Division, Oak Ridge National Laboratory, Oak Ridge, Tennessee 37831, United States

[§]Department of Chemistry, University of Tennessee, Knoxville, Tennessee 37996, United States

Supporting Information

ABSTRACT: Polystyrene of different molecular weights and their binary mixtures are studied in terms of their various mechanical responses to uniaxial compression at different temperatures. PS of M_w = 25 kg/mol is completely brittle until it is above its glass transition temperature T_g. In contrast, upon incorporation of a high molecular weight component, PS mixtures turn from barely ductile a few degrees below its T_g to ductile over 40° below T_g. In the upper limit, a PS of M_w = 319 kg/mol yields and undergoes plastic flow, even at T = −70 °C. The observed dependence of mechanical responses on molecular weight and molecular weight distribution can be adequately rationalized by the idea that yielding and plastic compression are caused by chain networking.

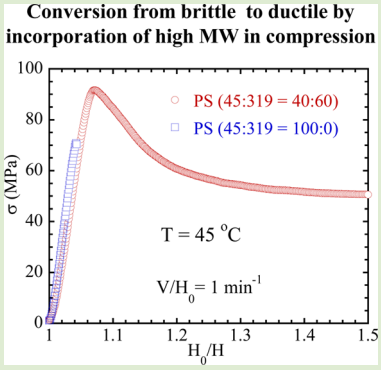

Polymeric glasses of high molecular weight undergo brittle-ductile transition (BDT) during continuous tensile extension. On the other hand, brittle failure in uniaxial compression has rarely been reported of polymer glasses. Polystyrene (PS) of high molecular weight undergoes a BDT around 70 °C in uniaxial extension, but is only known to be ductile during uniaxial compression.[1−14] Since nonpolymeric organic glasses are brittle in both uniaxial extension and compression, molecular weight is an important variable. Brittle tensile strength of polymer glasses drops sharply with decreasing molecular weight below a threshold value.[15−21] Much less is known about whether BDT occurs in compression. To explain the BDT phenomenon in extension, different accounts have been put forward, including the Ludwik[22]−Davidenov−Wittman[23]−Orowan[24] (LDWO) hypothesis, the correlation between primary[25] or secondary relaxation[26,27] and BDT, the relationship between entanglement density and crazing behavior,[21,28−32] considerations that relate the degree of strain hardening versus softening to the ductility of polymer glasses,[7−9,33−36] as well as fracture mechanical considerations.[37−39] These efforts, summarized in several monographs,[37,40−42] have formed a vast background for the subject of mechanical behavior of polymer glasses. Nevertheless, a coherent zeroth-order molecular picture was still missing about how and why only polymer glasses of sufficiently high molecular weight can yield and deform plastically well below their glass transition temperature T_g. Regarding polymer glasses as a structural hybrid made of a primary structure due to intersegmental (van der Waals) interactions and a chain network due to intermolecular uncrossability, a recent study[43] attempted to rationalize the observed stress σ_{BD} at the BDT in terms of breakdown of the chain network due to chain pullout and offers a plausible explanation of the molecular origin of BDT.

Many past theoretical studies[31,44−54] and computer simulations[44,55−76] have attempted to describe yielding behavior of such glassy polymers as PS and PMMA by comparing with experimental data[1−13,30] that are mostly based on uniaxial compression.[77] In these treatments, the phenomenological Eyring idea[78,79] offers an essential insight: The external deformation reduces the energy barrier against segmental hopping, causing the α-relaxation time τ_α to decrease rapidly so that dynamic yielding can take place. It is rarely addressed why large deformation could rejuvenate polymer glasses to produce Eyring-like yielding. Since typical compression experiments involve PS and PMMA of sufficiently high molecular weight, the lack of molecular weight effects has often been used as a validation that yielding is only controlled by molecular motions on a segmental scale.

This Letter explores when mechanical responses to uniaxial compression of several PS samples turn from ductile to brittle at different temperatures. The data reveal that the molecular weight and molecular weight distribution play specific roles. Contrasting a monodisperse PS25K of M_w = 25 kg/mol that is brittle under compression even just 1° below its T_g = 96 °C, PS319K of high molecular weight is ductile all the way down to 178 °C below its T_g = 108 °C. A third sample of PS45K is a

Received: July 1, 2015
Accepted: September 2, 2015
Published: September 9, 2015

DOI: 10.1021/acsmacrolett.5b00442
ACS Macro Lett. 2015, 4, 1072−1076

50:50 mixture of high $M_L \approx 100$ kg/mol and low $M_S \approx 2$ kg/mol (PS2K) and can turn ductile upon approaching its $T_g \sim 59$ °C. A fourth PS(45:319) is a mixture of PS319K and PS45K at a weight ratio of 60:40%. This mixture can resist brittle failure at least 40° below its T_g = 86 °C. The detailed molecular, viscoelastic characteristics and sample preparation procedures of these four samples are provided in the Supporting Information (SI), including the DSC information on these PS samples. Experimental protocols and the apparatus are also discussed in the SI.

Before presenting the various experimental results, we emphasize the need to conduct real-time visualization in order to characterize the nature of the mechanical response of any polymer glasses under uniaxial compression. Compression is different from extension in many ways, although both can increase segmental mobility to produce yielding, as shown in computer simulation.[75] In our view, principal difference is as follows. During displacement-controlled tensile extension, the emergent stress transmits along the stretching direction; different sections of the specimen bear the same load. In other words, the loading elements are mechanically and structurally in series. In compression, they are in parallel and therefore independent of one another. Thus, compression is more tolerant of imperfections due to either man-made flaws or structural defects or nonideal lubrication. Because of the difference, compressive stress versus strain curves may not explicitly reveal whether brittle failure has taken place.

We begin our investigation by documenting a remarkable brittle response of PS25K to uniaxial compression. Figure 1

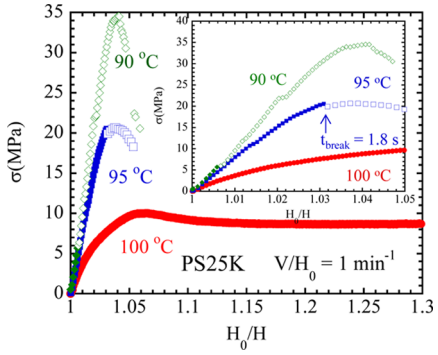

Figure 1. Stress vs strain curves from uniaxial compression of PS25K at three temperatures, showing brittle responses at both $(T_g - 6)$ and $(T_g - 1)$ °C and ductile at $(T_g + 4)$ °C. The open symbols show measurements after macroscopic failure has taken place. The inset blow-up indicates that PS25K is already above T_g at 100 °C.

shows that PS25K is brittle, even at $(T_g - 1)$ °C and turns ductile at $(T_g + 4)$ °C. To demonstrate the difference, we have provided two movies (PS25K-95C and PS25K-100C) as SI. The reduced Young's modulus read from the initial slope of the inset figure also confirms that PS25K is no longer glassy at $(T_g + 4)$ °C. It is necessary to note that, despite the brittle failure, the compressive stress can still climb, even showing a peak, which could be mistaken as a sign of yielding had we not taken video recording to observe the brittle breakdown of the specimen.

In contrast, PS319 is entirely ductile, as shown in Figure 2. The stress versus strain curves exhibit pronounced peaks as a sign of yielding followed by plastic flow. A movie (PS319K-20C) in the SI shows the ductile compression at room temperature. The sample also undergoes ductile compression at

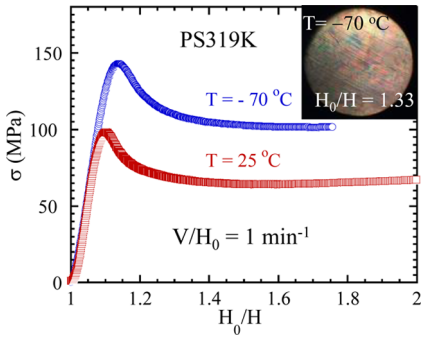

Figure 2. Stress vs strain curves from uniaxial compression of PS319K at two temperatures, both showing ductile response. Inset is a photo of the cross-section of the specimen after 33% compression (i.e., H_0/H = 1.33) at $(T_g - 178)$ °C.

$(T_g - 178)$ °C, essentially free of any visible failure up to a compression ratio H_0/H of 1.33, as shown by the inset photo in Figure 2. It is worth noting that the same PS319K is entirely brittle in extension at the same rate at room temperature, let alone $(T_g - 178)$ °C.

In passing, one comment is in order. Although the difference between PS25K and PS319K can be treated as something to expect from empirical knowledge, the current understanding and theoretic treatment do not rationalize why long chains in PS319K ensure ductile response in compression yet still cannot prevent brittle failure in extension.

We collect more experimental information by turning to another sample. PS45K is a binary mixture with $Z = (M_L/M_e)(0.5)^{1.2-1.3} = 3$ entanglements per chain according to the rheological definition of entanglement,[80] where M_e = 13 kg/mol for PS. The small-amplitude oscillatory shear (SAOS) data in the SI confirm that PS45K is hardly entangled. At what temperature would this sample undergo ductile compression? To answer this question, Figure 3 presents the stress versus strain curves at various temperatures. The movie (PS45K-50C) in the SI indicates that PS45K is brittle at and below 50 °C. In comparison, the movie (PS45K-55C) appears to show ductile compression at 55 °C. Consistently, the Young's modulus E

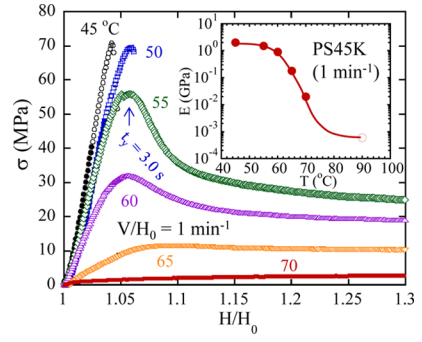

Figure 3. Stress vs strain curves from uniaxial compression of PS45K at six temperatures with V/H_0 = 1 min^{-1}. The responses are brittle at 45 and 50 °C, where open circles and squares are measurements after macroscopic failure has taken place. The response is ductile at and above 55 °C. At 1 min^{-1}, the Young's modulus E shows noticeable decrease at and above 60 °C and diminishes at 70 °C. The inset shows E as a function of temperature to reveal the broad glass transition on the time scale set by the compressional rate of 1 min^{-1}, where the extrapolated open circle represents the melt elastic modulus E of PS at 0.6 MPa.

DOI: 10.1021/acsmacrolett.5b00442
ACS Macro Lett. 2015, 4, 1072−1076

decreases with temperature, as shown in the inset of Figure 3. The glass transition behavior indicated by such DMA-like data is consistent with the DSC data presented in the SI, which describes a broad glass transition between 54 and 67 °C. Thus, the ductile response of PS45 at 55 °C is perhaps not surprising, although the stress versus strain curve suggests that PS45K is still glassy at 55 °C.

To explore the relationship between plastic compression and segmental dynamics, we carry out several complementary tests, such as stress relaxation, SAOS, and dielectric spectroscopic measurements.[81−84] The stress relaxation behavior from 2% compression in the elastic deformation regime shows in Figure 4 that PS45K relaxes very slowly at 45 °C and speeds up considerably at 55 °C. In particular, a KWW fit of $\sigma/\sigma_0 = \exp[-(t/\tau_\alpha)^\beta]$[85] to the data gives the segmental relaxation time τ_α and β, as presented in Table 1. Consistent with the stress relaxation data in Figure 4, the SAOS data in the SI shows that the storage modulus G' rises to equal loss modulus G'' at accessible frequencies ω_α, listed in Table 1 as $\tau_\alpha = 1/\omega_\alpha$ for comparison. Figure 5 shows the Arrhenius temperature dependence of τ_α. The data extracted from dielectric measurements show similar temperature dependence.[81−84] According to both Figure 4 and Figure 5, τ_α of PS45K is at least 16 s at 55 °C in the absence of any large deformation.

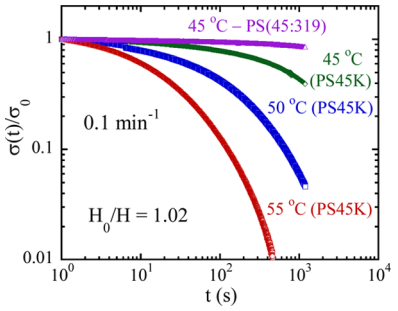

Figure 4. Stress relaxation from small uniaxial compression (at H_0/H = 1.02) of PS45K at T = 45, 50, and 55 °C and PS(45:319) at 45 °C, where the data are presented by choosing the onset time t_0 to be 1 s. The preyield compression was produced at a rate of $V/H_0 = 0.1$ min^{-1}. The relaxation for the PS(45:319) mixture (purple color online) is much slower because of its higher T_g than that of PS45K.

Equipped with the explicit information on segmental mobility, we further examine the compression behavior at 55 °C. At the rate of 1 min^{-1}, it takes just t_y = 3.0 s to reach the yield point at 5% compression, as shown in Figure 3. For plastic deformation to take place beyond 5%, as shown by diamonds in Figure 3 and movie in SI (PS45-55C), presumably the compression has reduced the potential barrier height to enable segmental hopping. In other words, the observed dynamic yielding implies that segmental mobility is much greater than what can be characterized by τ_α = 16 s. For comparison, we have also performed SAOS measurements of τ_α for PS25K, as summarized in Figure 5. At $(T_g - 1)$ °C, PS25K has a short α-time τ_α of only 0.9 s. Yet, the compression of PS45K is brittle

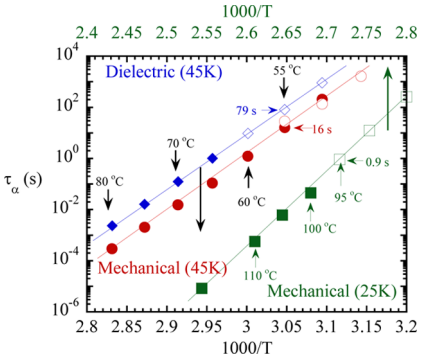

Figure 5. α-Relaxation time τ_α, as determined by mechanical (circles and squares) and dielectric (diamonds) measurements, as well as the KWW fitting to the stress relaxation behavior in Figure 4, as a function of $1000/T$ for PS45K and PS25K, where the open diamonds and square are extrapolated, based on the revealed Arrhenius behavior. Circles and diamonds are plotted against the lower X axis, and squares are plotted against the upper X axis. The open circles are the dominant relaxation times from the stress relaxation data. Solid lines are added to show the revealed Arrhenius dependence.

even though it takes t_{break} = 1.8 s > τ_α = 0.9 s for the failure to take place. Thus, the contrast between PS45K and PS25K is rather striking.

Although PS45K is a 50:50 mixture of high and low T_g components, 100 and 29 °C, respectively, its overall preyield segmental dynamics are rather slow. According to Figure 4, the stress only decreases by 15% after 3.0 s, which is the time taken to yield at 55 °C, according to Figure 3. Most segments would be too slow to participate in any plastic deformation unless they have been mobilized somehow. How did segmental dynamics accelerate? Such acceleration clearly did not occur in PS25K during compression at $(T_g - 1)$ °C. Because PS25K shows brittle failure at $(T_g - 1)$ °C and ductile compression at $(T_g + 4)$ °C, we are inclined to suggest for polymer glasses of low molar mass that (a) the condition of $\tau_\alpha \ll t_y = \varepsilon_y/\dot{\varepsilon} < 1/10\dot{\varepsilon}$ is necessary for plastic deformation to take place since yielding typically occurs at $\varepsilon_y < 0.1$; (b) compression may not reduce τ_α appreciably in the absence of long chains. For PS45K, ductile compression occurs at 55 °C, although $\tau_\alpha \gg t_y$, suggesting the effective α-time $\tau_{\alpha(\text{eff})}$ was probably lowered during compression. There are two key factors to recognize. PS45K has (a) 50% long chains, and (b) the other 50% short chains have a lower T_g. Both factors favor a ductile response. It is plausible that long chains in PS45K caused yielding and plastic deformation at 55 °C.

To further probe the role of long chains, we reinforce PS45K with PS319 by making a binary mixture labeled as PS(45:319), made of 40% PS45K and 60% PS319K. The result is remarkable. Although its DSC data reveals the glass transition to take place at T_g = 86 °C, PS(45:319) is ductile at 45 °C, in sharp contrast to PS45K, as shown in Figure 6 and by comparison between the movie [PS(45:319)-45C] and the movie (PS45-55C) in the SI. Here it is important to note that stress relaxation of PS(45:319) is immeasurably slow, as shown

Table 1. α-Relaxation Time of PS45K at Different Temperatures

(T_g ~ 59 °C)	45 °C	50 °C	55 °C	60 °C	65 °C	70 °C
SAOS τ_α	250 s	16 s	1.2 s	0.1 s	0.015 s	
KWW τ_α	1640 s	134 s	28 s			
β	0.51	0.53	0.56			

DOI: 10.1021/acsmacrolett.5b00442
ACS Macro Lett. 2015, 4, 1072−1076

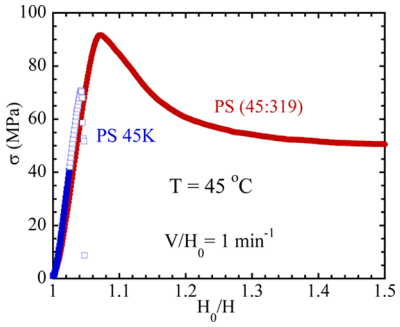

Figure 6. Stress vs strain curves from uniaxial compression of PS(46:319) and PS45K at T = 45 °C, with V/H_0 = 1 min^{-1}. PS45K is brittle, but upon incorporation of 60% PS319K, the mixture PS(45:319) has an even higher T_g and is yet completely ductile.

in Figure 4. However, because PS(45:319) has as many as Z = 15 entanglements per chain[86] according to the estimate given in the caption of Figure A.2 in SI, instead of Z = 3 for PS45K, it can resist brittle failure even at 45 °C, 44° below its T_g, where the α-time is many orders of magnitude longer than the deformation time. The fact that the compression of PS(45:319) is ductile indicates that $\tau_{\alpha(\mathrm{eff})}$ has become greatly reduced by the uniaxial compression. The same cannot be said for the compression of pure PS45K.

To explain why PS319K is brittle in extension and ductile in compression at room temperature, we recall a previous study documenting the suppression of brittle extension in PS by pressurization.[87] The pressure arising from compression makes PS319K more resistant against chain pullout. When high molecular weight fraction is deficient or absent, as in the respective cases of PS45K and PS25K, brittle failure is the only outcome, even in compression, until the temperature approaches or rises above T_g. In contrast, when either PS45K (as shown in Figure 6) or PS25K[88] is adequately reinforced by PS319K, the mixtures can be ductile significantly below T_g, although τ_α far exceeds the time scale associated with the compression rate.

In summary, we have studied four PS samples of different molecular weights and molecular weight distributions in terms of the variety of mechanical responses to uniaxial compression at different temperatures. In absence of long chains, PS behaves like a nonpolymeric organic glass, brittle even in compression until T_g, as shown by PS25K in Figure 1. The chance to exhibit ductile compression below T_g improves when 50% long chains of M_L = 100 kg/mol is present along with oligomeric PS of M_S = 2 k/mol. Brittle failure is largely suppressed when more long chains are added to make the mixture PS(45:319). Clearly, the ability of long PS chains to form a load-bearing network is required to attain plastic compression well below T_g. In short, the present observations indicate that high molecular weight is necessary in a glassy polymer to enable yielding and plastic deformation in compression. It can be expected that the same conclusion is valid to anticipate a full range of yielding and failure behavior involving compression of any other polymer glasses.

■ ASSOCIATED CONTENT

Supporting Information

The Supporting Information is available free of charge on the ACS Publications website at DOI: 10.1021/acsmacrolett.5b00442.

The detailed molecular and viscoelastic characteristics and sample preparation procedures of the four samples, including the DSC information on the PS samples; Experimental protocols and the apparatus are also discussed (PDF)

Movie of PS25K-95C in mpeg format (MPG)

Movie of PS25K-100C in mpeg format (MPG)

Movie of PS319K-20C in mpeg format (MPG)

Movie of PS45K-50C in mpeg format (MPG)

Movie of PS45K-55C in mpeg format (MPG)

Movie of PS(45:319)-45C in mpeg format (MPG)

All the movies involve the same rate of V/H_0 = 1 min^{-1}.

■ AUTHOR INFORMATION

Corresponding Author

*E-mail: swang@uakron.edu.

Notes

The authors declare no competing financial interest.

■ ACKNOWLEDGMENTS

This work is, in part, supported by NSF-DMR (EAGER-1444859) and the U.S. Department of Energy, Office of Science, Basic Energy Sciences, Materials Sciences and Engineering Division. We thank the reviewers for their encouraging comments.

■ REFERENCES

(1) Bauwens-Crowet, C.; Bauwens, J. C.; Homès, G. *J. Mater. Sci.* **1972**, *7*, 176−183.
(2) Boyce, M. C.; Parks, D. M.; Argon, A. S. *Mech. Mater.* **1988**, *7*, 15−33.
(3) Boyce, M. C.; Arruda, E. M. *Polym. Eng. Sci.* **1990**, *30*, 1288−1298.
(4) Arruda, E. M.; Boyce, M. C. *J. Mech. Phys. Solids* **1993**, *41*, 389−412.
(5) Hasan, O. A.; Boyce, M. C. *Polym. Eng. Sci.* **1995**, *35*, 331−344.
(6) Capaldi, F. M.; Boyce, M. C.; Rutledge, G. C. *Polymer* **2004**, *45*, 1391−1399.
(7) Engels, T. T.; Govaert, L. L.; Meijer, H. H. Mechanical characterization of glassy polymers: quantitative prediction of their short- and long-term responses. In *Polymer Science: A Comprehensive Reference*; Matyjaszewski, K., Möller, M., Eds.; Elsevier: Amsterdam, 2012; Vol 2, p 723.
(8) Senden, D. J. A.; Krop, S.; van Dommelen, J. A. W.; Govaert, L. E. *J. Polym. Sci., Part B: Polym. Phys.* **2012**, *50*, 1680−1693.
(9) van Breemen, L. C. A.; Engels, T. A. P.; Klompen, E. T. J.; Senden, D. J. A.; Govaert, L. E. *J. Polym. Sci., Part B: Polym. Phys.* **2012**, *50*, 1757−1771.
(10) Wu, J. J.; Buckley, C. P. *J. Polym. Sci., Part B: Polym. Phys.* **2004**, *42*, 2027−2040.
(11) Nanzai, Y. *Prog. Polym. Sci.* **1993**, *18*, 437−479.
(12) Yoshizawa, M.; Ohsawa, H. *J. Mater. Process. Technol.* **1997**, *68*, 206−214.
(13) Nanzai, Y.; Yamasaki, T.; Yoshioka, S. y. *JSME Int. J., Ser. A* **1998**, *41*, 31−39.
(14) Lin, P.; Cheng, S.; Wang, S.-Q. *ACS Macro Lett.* **2014**, *3*, 784−787.
(15) Vincent, P. *Polymer* **1960**, *1*, 425−444.
(16) White, E. F. T.; Murphy, B. M.; Haward, R. N. *J. Polym. Sci., Part B: Polym. Lett.* **1969**, *7*, 157−160.
(17) Haward, R. N.; Brough, I. *Polymer* **1969**, *10*, 724−736.
(18) Gent, A. N.; Thomas, A. G. *Journal of Polymer Science Part A-2: Polymer Physics* **1972**, *10*, 571−573.
(19) Fellers, J. F.; Kee, B. F. *J. Appl. Polym. Sci.* **1974**, *18*, 2355−2365.
(20) Kusy, R. P.; Turner, D. T. *Polymer* **1974**, *15*, 394−395.
(21) Kramer, E. *J. Mater. Sci.* **1979**, *14*, 1381−1388.

DOI: 10.1021/acsmacrolett.5b00442
ACS Macro Lett. 2015, 4, 1072−1076

(22) Ludwik, P. Z. *Ver. Deut. Ing* **1927**, *71*, 1532.
(23) Davidenkov, N. N.; Wittman, F. *Phys. Technol. Znst. (USSR)* **1937**, *4*, 300.
(24) Orowan, E. *Rep. Prog. Phys.* **1949**, *12*, 185.
(25) Aharoni, S. M. *J. Appl. Polym. Sci.* **1972**, *16*, 3275−3284.
(26) Wu, S. *J. Appl. Polym. Sci.* **1992**, *46*, 619−624.
(27) Chen, L. P.; Yee, A. F.; Moskala, E. J. *Macromolecules* **1999**, *32*, 5944−5955.
(28) Donald, A. M.; Kramer, E. J. *J. Polym. Sci., Polym. Phys. Ed.* **1982**, *20*, 899−909.
(29) Kramer, E. J. *Adv. Polym. Sci.* **1983**, *52*−*3*, 1−56.
(30) De Focatiis, D. S. A.; Buckley, C. P.; Hutchings, L. R. *Macromolecules* **2008**, *41*, 4484−4491.
(31) De Focatiis, D. S. A.; Embery, J.; Buckley, C. P. *J. Polym. Sci., Part B: Polym. Phys.* **2010**, *48*, 1449−1463.
(32) De Focatiis, D. S. A.; Buckley, C. P. *Polymer* **2011**, *52*, 4045−4053.
(33) van Melick, H. G. H.; Govaert, L. E.; Meijer, H. E. H. *Polymer* **2003**, *44*, 2493−2502.
(34) Tervoort, T.; Govaert, L. *J. Rheol.* **2000**, *44*, 1263.
(35) Govaert, L. E.; Tervoort, T. A. *J. Polym. Sci., Part B: Polym. Phys.* **2004**, *42*, 2041−2049.
(36) Senden, D. J. A.; van Dommelen, J. A. W.; Govaert, L. E. *J. Polym. Sci., Part B: Polym. Phys.* **2010**, *48*, 1483−1494.
(37) Williams, J. G. *Fracture Mechanics of Polymers*; Halsted Press (Ellis Horwood Limited): New York, 1987.
(38) Kramer, E.; Berger, L. Fundamental processes of craze growth and fracture. In *Crazing in Polymers, Vol. 2*; Kausch, H., Ed.; Springer: Berlin/Heidelberg, 1990; Vol. *91*, pp 1−68.
(39) Lesser, A. J., Fatigue Behavior of Polymers. *Encyclopedia of Polymer Science and Technology*; John Wiley & Sons, Inc.: New York, 2002.
(40) Haward, R. N.; Young, R. J. *The Physics of Glassy Polymers*; Springer: Netherlands, 1997.
(41) Ward, I. M.; Sweeney, J. *Mechanical Properties of Solid Polymers*; Wiley: New York, 2012.
(42) Argon, A. S. *The Physics of Deformation and Fracture of Polymers*; Cambridge University Press: New York, 2013.
(43) Wang, S.-Q.; Cheng, S.; Lin, P.; Li, X. *J. Chem. Phys.* **2014**, *141*, 094905.
(44) Klompen, E. T. J.; Engels, T. A. P.; Govaert, L. E.; Meijer, H. E. H. *Macromolecules* **2005**, *38*, 6997−7008.
(45) Klompen, E. T. J.; Engels, T. A. P.; van Breemen, L. C. A.; Schreurs, P. J. G.; Govaert, L. E.; Meijer, H. E. H. *Macromolecules* **2005**, *38*, 7009−7017.
(46) Brader, J. M.; Cates, M. E.; Fuchs, M. *Phys. Rev. Lett.* **2008**, *101*, 138301.
(47) Brader, J. M.; Voigtmann, T.; Fuchs, M.; Larson, R. G.; Cates, M. E. *Proc. Natl. Acad. Sci. U. S. A.* **2009**, *106*, 15186−15191.
(48) Chen, K.; Saltzman, E. J.; Schweizer, K. S. *J. Phys.: Condens. Matter* **2009**, *21*, 503101.
(49) Chen, K.; Saltzman, E. J.; Schweizer, K. S. *Annu. Rev. Condens. Matter Phys.* **2010**, *1*, 277−300.
(50) Chen, K.; Schweizer, K. S. *Macromolecules* **2008**, *41*, 5908−5918.
(51) Chen, K.; Schweizer, K. S. *Phys. Rev. E* **2008**, *78*, 031802.
(52) Chen, K.; Schweizer, K. S. *Phys. Rev. Lett.* **2009**, *102*, 038301.
(53) Chen, K.; Schweizer, K. S. *Phys. Rev. E* **2010**, *82*, 041804.
(54) Chen, K.; Schweizer, K. S. *Macromolecules* **2011**, *44*, 3988−4000.
(55) Lyulin, A. V.; Balabaev, N. K.; Mazo, M. A.; Michels, M. A. J. *Macromolecules* **2004**, *37*, 8785−8793.
(56) Lyulin, A. V.; Vorselaars, B.; Mazo, M. A.; Balabaev, N. K.; Michels, M. A. J. *Europhys. Lett.* **2005**, *71*, 618−624.
(57) Lyulin, A. V.; Michels, M. A. J. *J. Non-Cryst. Solids* **2006**, *352*, 5008−5012.
(58) Lyulin, A. V.; Michels, M. A. J. *Phys. Rev. Lett.* **2007**, *99*, 085504.
(59) Vorselaars, B.; Lyulin, A. V.; Michels, M. A. J. *Macromolecules* **2009**, *42*, 5829−5842.
(60) Vorselaars, B.; Lyulin, A. V.; Michels, M. A. J. *J. Chem. Phys.* **2009**, *130*, 074905.
(61) Balabaev, N. K.; Mazo, M. A.; Lyulin, A. V.; Oleinik, E. F. *Polym. Sci., Ser. A* **2010**, *52*, 633−644.
(62) Barrat, J.-L.; Baschnagel, J.; Lyulin, A. *Soft Matter* **2010**, *6*, 3430−3446.
(63) Hoy, R. S.; Robbins, M. O. *J. Polym. Sci., Part B: Polym. Phys.* **2006**, *44*, 3487−3500.
(64) Hoy, R. S.; Robbins, M. O. *Phys. Rev. Lett.* **2007**, *99*, 117801.
(65) Hoy, R. S.; Robbins, M. O. *Phys. Rev. E* **2008**, *77*, 031801.
(66) Hoy, R. S.; Robbins, M. O. *J. Chem. Phys.* **2009**, *131*, 244901.
(67) Hoy, R. S.; O'Hern, C. S. *Phys. Rev. E* **2010**, *82*, 041803.
(68) Hoy, R. S. *J. Polym. Sci., Part B: Polym. Phys.* **2011**, *49*, 979−984.
(69) Tervoort, T. A.; Klompen, E. T. J.; Govaert, L. E. *J. Rheol.* **1996**, *40*, 779−797.
(70) van Breemen, L. C. A.; Engels, T. A. P.; Pelletier, C. G. N.; Govaert, L. E.; den Toonder, J. M. J. *Philos. Mag.* **2009**, *89*, 677−696.
(71) Nayak, K.; Read, D. J.; McLeish, T. C. B.; Hine, P. J.; Tassieri, M. *J. Polym. Sci., Part B: Polym. Phys.* **2011**, *49*, 920−938.
(72) van Breemen, L. C. A.; Klompen, E. T. J.; Govaert, L. E.; Meijer, H. E. H. *J. Mech. Phys. Solids* **2011**, *59*, 2191−2207.
(73) Fielding, S.; Moorcroft, R.; Larson, R.; Cates, M. *J. Chem. Phys.* **2013**, *138*, 12A504.
(74) Jatin; Sudarkodi, V.; Basu, S. *Int. J. Plast.* **2014**, *56*, 139−155.
(75) Riggleman, R. A.; Toepperwein, G. N.; Papakonstantopoulos, G. J.; de Pablo, J. J. *Macromolecules* **2009**, *42*, 3632−3640.
(76) Riggleman, R. A.; Lee, H.-N.; Ediger, M.; De Pablo, J. J. *Soft Matter* **2010**, *6*, 287−291.
(77) Brittle polymer glasses, such as PS, can hardly yield in tensile extension until the temperature approaches T_g = 100 °C. Therefore, compression is the commonly used mode to explore yielding characteristics, e.g., yield stress as a function of temperature and deformation rate.
(78) Eyring, H. *J. Chem. Phys.* **1936**, *4*, 283−291.
(79) Tobolsky, A.; Eyring, H. *J. Chem. Phys.* **1943**, *11*, 125−134.
(80) Colby, R. H.; Rubinstein, M. *Macromolecules* **1990**, *23*, 2753−2757.
(81) Pakula, T.; Geyler, S.; Edling, T.; Boese, D. *Rheol. Acta* **1996**, *35*, 631−644.
(82) Roland, C. M.; Ngai, K. L.; Santangelo, P. G.; Qiu, X. H.; Ediger, M. D.; Plazek, D. J. *Macromolecules* **2001**, *34*, 6159−6160.
(83) Pakula, T. Dielectric and mechanical spectroscopy: A comparison. In *Broadband Dielectric Spectroscopy*; Kremer, F., Schönhals, A., Eds.; Springer: Berlin; Heidelberg, 2003; pp 597−623.
(84) Ngai, K. *Relaxation and Diffusion in Complex Systems*; Springer Science & Business Media: New York, 2011.
(85) Williams, G.; Watts, D. C. *Trans. Faraday Soc.* **1970**, *66*, 80−85.
(86) For convenience, the ability to form a chain network has been indicated here in terms of chain entanglement. See ref 43 for a discussion of the difference between chain and entanglement networks.
(87) Matsushige, K.; Radcliffe, S. V.; Baer, E. *J. Appl. Polym. Sci.* **1976**, *20*, 1853−1866.
(88) Liu, J. N.; Wang, S. Q., unpublished.

DOI: 10.1021/acsmacrolett.5b00442
ACS Macro Lett. 2015, 4, 1072−1076